

ELECTRIC FIELD MODELING OF OUTDOOR INSULATOR FOR OPTIMIZED PERFORMANCE

MOHD HAYUMABDISSALAM BIN TALI @ RAZALI

A project report submitted in partial fulfillment of the
requirement for the award of the
Degree of Master of Electrical Engineering

Faculty of Electrical and Electronic Engineering
University Tun Hussein Onn Malaysia

JANUARY 2014

ABSTRACT

This project presents the study of electric field stress along the surface of a 132 kV ceramic post insulator. Insulators are among the important devices of the electric power transmission systems. They are used to support and separate conductors at high voltage. Different insulator shapes have been obtained by varying several parameters, which defines the shape of the post insulator. For each insulator shape, the maximum electric field stress occurring on the insulator surface has been determined under clean and dry environment. The COMSOL Multiphysics software has been employed to investigate the electric field stress along the insulator's surface. The full detailed model of a dry and clean ceramic 132kV post insulator with 25 sheds has been developed for the base model calculation. The maximum value of electric field stress was found to be at the junction between the porcelain and the end fitting. End fittings with round edges tend to reduce the electric field stress along the insulator's surface. With smaller first shed's outer corner radius, the electric field stress slightly decreases. The electric field stress of the 25th shed near the top end fitting tends to reduce as the shed's inclination angle is increased. Furthermore, as the shed's diameter increases, the electric field stress increases except at the shed's outer corner where the electric field stress decreases. With greater distance between the first shed and the bottom end fitting, the electric field stress becomes lower. The end fittings design was found to be significantly affecting the electric field stress along the surface of the post insulator. A modified post insulator is proposed and proven to have a better performance in term of electric field stress.

ABSTRAK

Projek ini membentangkan tentang kajian tekanan medan electric di sepanjang permukaan sebuah penebat pos seramik 132kV. Penebat adalah salah satu alat penting dalam system penghantaran kuasa elektrik. Ia digunakan untuk menampung dan memisahkan konduktor pada voltan tinggi. Bentuk penebat yang berbeza telah dicapai dengan mempelbagaikan beberapa parameter yang mentakrifkan bentuk pos penebat. Untuk setiap bentuk penebat, tekanan medan elektrik maksimum yang terjadi di permukaan penebat telah ditentukan di dalam persekitaran yang bersih dan kering. Peisian COMSOL Multiphysics telah digunakan untuk menyiasat tekanan medan elektrik di sepanjang permukaan insulator. Sebuah model penebat pos seramik 132kV yang terperinci yang kering dan bersih telah dimajukan untuk kiraan model asas. Tekanan medan elektrik yang maksimum telah didapati berada di simpang antara porselin dan sambungan hujung. Sambungan hujung yang mempunyai bucu yang bulat cenderung untuk mengurangkan tekanan medan elektrik di permukaan penebat. Dengan jejari luar 'shed' pertama yang kecil, tekanan medan elektrik berkurangan sedikit. Tekanan medan elektrik 'shed' yang ke-25 berhampiran sambungan hujung atas cenderung untuk berkurang apabila sudut kecenderungan shed bertambah. Tambahan pula, apabila diameter 'shed' menaik, tekanan medan elektrik menaik kecuali di bahagian bucu luar 'shed' yang mana tekanan medan elektrik berkurang. Dengan jarak yang semakin jauh antara 'shed' yang pertama dan sambungan hujung bawah, tekanan medan elektrik berkurang. Rekabentuk sambungan hujung memberi kesan yang besar kepada tekanan medan elektrik di sepanjang permukaan penebat. Sebuah penebat pos yang telah dimodifikasi telah diuarkan dan telah terbukti mempunyai persembahan yang lebih mantap dari segi tekanan medan elektrik.

CONTENTS

| | |
|---|-----|
| TITLE | i |
| STUDENT'S DECLARATION | ii |
| DEDICATION | iii |
| ACKNOWLEDGEMENT | iv |
| ABSTRACT | v |
| CONTENTS | vii |
| LIST OF FIGURES | xi |
| LIST OF TABLES | xii |
| LIST OF APPENDICES | xiv |
| LIST OF SYMBOLS AND ABBREVIATIONS | xvi |
| CHAPTER 1 | |
| INTRODUCTION | |
| 1.1 Introduction | 1 |
| 1.2 Problem statement | 2 |
| 1.3 Objectives | 3 |
| 1.4 Scope of the project | 3 |
| CHAPTER 2 | |
| REVIEW OF LITERATURE | |
| 2.1 Overview | 4 |
| 2.2 Ceramic insulator | 9 |
| 2.3 Electric field stress | 10 |
| 2.4 Numerical electric field analysis methods | 12 |

| | | |
|-------|--|----|
| 2.4.1 | Finite element method | 14 |
| 2.5 | Factors influencing the electric field stress on insulator | 18 |
| 2.5.1 | Shape of insulator | 18 |
| 2.5.2 | Corona ring application | 20 |
| 2.5.3 | Permittivity of the material | 22 |
| 2.5.4 | Potential difference | 23 |
| 2.5.5 | External influences | 23 |
| 2.6 | Effect of electric field stress on insulator | 24 |
| 2.6.1 | Corona discharge | 24 |
| 2.6.2 | Flashover | 25 |

CHAPTER 3 METHODOLOGY

| | | |
|-------|--------------------|----|
| 3.1 | Overview | 27 |
| 3.2 | Simulation process | 29 |
| 3.2.1 | Phase 1 | 30 |
| 3.2.2 | Phase 2 | 30 |
| 3.2.3 | Phase 3 | 31 |

CHAPTER 4 RESULT AND DATA ANALYSIS

| | | |
|-------|---|----|
| 4.1 | Overview | 32 |
| 4.2 | Simulation of 132kV post insulator | 32 |
| 4.2.1 | Properties of materials | 33 |
| 4.2.2 | Boundary condition | 34 |
| 4.2.3 | Meshing | 34 |
| 4.2.4 | Electric field simulation | 35 |
| 4.3 | Effects of the distance between the first shed and the bottom end fitting | 42 |

| | | |
|-----|---------------------------------------|----|
| 4.4 | Effects of shed's diameter | 48 |
| 4.5 | Effects of shed's inclination angle | 55 |
| 4.6 | Effects of shed's outer corner radius | 61 |
| 4.7 | Effects of end fittings design | 67 |
| 4.8 | Effects of modification on first shed | 71 |
| 4.9 | Proposed model | 75 |

CHAPTER 5 CONCLUSION AND RECOMMENDATION

| | | |
|-----|---------------------------------|----|
| 5.1 | Overview | 83 |
| 5.2 | Conclusion | 83 |
| 5.3 | Recommendation and future works | 85 |

| | |
|-------------------|-----------|
| REFERENCES | 86 |
|-------------------|-----------|



LIST OF FIGURES

| | | |
|-----|--|----|
| 2.1 | Typical constructions of ceramic type suspension insulators | 10 |
| | a) Standard | 10 |
| | b) Open profile (self-cleaning) | 10 |
| | c) Anti-fog and for DC applications | 10 |
| 2.2 | Illustration of electric field | 11 |
| 2.3 | Triangular and tetrahedron shaped finite discrete elements. | 16 |
| 2.4 | a) Examples of the electric field distribution surrounding the composite insulator end fitting of Design 1 | 20 |
| | b) Examples of the electric field distribution surrounding the composite insulator end fitting of Design 2 | 20 |
| | c) Examples of the electric field distribution surrounding the composite insulator end fitting of Design 3 | 20 |
| 2.5 | a) Potential distributions on insulator with corona ring | 21 |
| | b) Potential distributions on insulator without corona ring | 21 |
| 2.6 | Corona discharge activities on insulator | 25 |
| 3.1 | Overall flowchart of the project | 28 |
| 3.2 | Flowchart of the simulation process | 29 |
| 4.1 | a) Drawn model of 132kV post insulator | 33 |
| | b) Actual model of 132kV post insulator | 33 |

| | | |
|------|--|----|
| 4.2 | a) Boundary condition of the base model insulator at voltage terminal | 34 |
| | b) Boundary condition of the base model insulator at ground terminal | 34 |
| 4.3 | Meshing of the insulator model | 35 |
| 4.4 | Electric field stress of 132kV post insulator | 36 |
| 4.5 | The line of measurement along the surface of porcelain of 132kV post insulator | 36 |
| 4.6 | Zone division of the 132 kV post insulator | 37 |
| 4.7 | Points of interest in Zone I | 38 |
| 4.8 | Points of interest in Zone II | 38 |
| 4.9 | Points of interest in Zone III | 39 |
| 4.10 | Electric field stress along the 132kV post insulator's surface | 39 |
| 4.11 | Electric field stress in Zone I | 40 |
| 4.12 | Electric field stress in Zone II | 40 |
| 4.13 | Electric field stress in Zone III | 41 |
| 4.14 | Distance between the first shed to bottom end fitting | 42 |
| 4.15 | Electric field stress in Zone I with different first shed to bottom end fitting distance | 42 |
| 4.16 | Electric field stress in Zone II with different first shed to bottom end fitting distance | 43 |
| 4.17 | Electric field stress in Zone III with different first shed to bottom end fitting distance | 43 |
| 4.18 | Changes in electric field in Zone I as the distance between the first shed and bottom end fitting was varied | 45 |

| | | |
|------|---|----|
| 4.19 | Changes in electric field in Zone II as the distance between the first shed and bottom end fitting was varied | 46 |
| 4.20 | Changes in electric field stress in Zone III as the distance between the first shed and bottom end fitting was varied | 47 |
| 4.21 | Shed's diameter of 132 kV post insulator | 48 |
| 4.22 | Electric field stress in Zone I with different shed's diameter | 49 |
| 4.23 | Electric field stress in Zone II with different shed's diameter | 49 |
| 4.24 | Electric field stress in Zone III with different shed's diameter | 50 |
| 4.25 | Changes in electric field stress in Zone I as the shed's diameter was varied | 51 |
| 4.26 | Changes in electric field stress in Zone II as the shed's diameter was varied | 53 |
| 4.27 | Changes in electric field stress in Zone III as the shed's diameter was varied | 54 |
| 4.28 | Inclination angle of 132 kV post insulator | 55 |
| 4.29 | Electric field stress in Zone I with different shed's inclination angle | 55 |
| 4.30 | Electric field stress in Zone II with different shed's inclination angle | 56 |
| 4.31 | Electric field stress in Zone III with different shed's inclination angle | 56 |
| 4.32 | Changes in electric field stress in Zone I as inclination angle was varied | 57 |

| | | |
|------|---|----|
| 4.33 | Changes in electric field stress in Zone II as inclination angle was varied | 59 |
| 4.34 | Changes in electric field stress in Zone III as inclination angle was varied | 60 |
| 4.35 | Shed's outer corner radius of post insulator | 61 |
| 4.36 | Electric field stress in Zone I with different shed's outer corner radius | 61 |
| 4.37 | Electric field stress in Zone II with different shed's outer corner radius | 62 |
| 4.38 | Electric field stress in Zone III with different shed's outer corner radius | 62 |
| 4.39 | Changes in electric field stress in Zone I as shed's outer corner radius was varied | 63 |
| 4.40 | Changes in electric field stress in Zone II as shed's outer corner radius was varied | 65 |
| 4.41 | Changes in electric field stress in Zone III as shed's outer corner radius was varied | 66 |
| 4.42 | a) Bottom end fitting of base model | 67 |
| | b) Top end fitting of base model | 67 |
| 4.43 | a) Bottom end fitting Design A | 67 |
| | b) Top end fitting Design A | 67 |
| 4.44 | a) Bottom end fitting Design B | 67 |
| | b) Top end fitting Design B | 67 |
| 4.45 | a) Bottom end fitting Design C | 68 |
| | b) Top end fitting Design C | 68 |
| 4.46 | Electric field stress in Zone I with different end fittings design | 68 |

| | | |
|------|--|----|
| 4.47 | Electric field stress in Zone II with different end fittings design | 68 |
| 4.48 | Electric field stress in Zone III with different end fittings design | 69 |
| 4.49 | First shed Design A | 72 |
| 4.50 | First shed Design B (no shed). | 72 |
| 4.51 | Electric field stress in Zone I with different first shed design | 72 |
| 4.52 | Electric field stress In Zone II with different first shed design | 73 |
| 4.53 | Electric field stress In Zone III with different first shed design | 73 |
| 4.54 | Proposed model of 132 kV post insulator | 77 |
| 4.55 | Electric field stress of base model of 132kV post insulator | 78 |
| 4.56 | Electric field stress of proposed model of 132kV post insulator | 79 |
| 4.57 | Electric field stress in Zone I | 80 |
| 4.58 | Electric field stress in Zone II | 80 |
| 4.59 | Electric field stress in Zone III | 81 |

LIST OF TABLES

| | | |
|------|---|----|
| 2.1 | Journals referred in doing the project | 5 |
| 2.2 | Brief explanation on the numerical method to calculate electric field | 12 |
| 2.3 | Relative permittivity of material | 22 |
| 4.1 | Dimension of 132kV post insulator | 33 |
| 4.2 | Relative permittivity of the insulator's material | 34 |
| 4.3 | Electric field stress at points of interest for 1332kV post insulator | 41 |
| 4.4 | Electric field stress at point A, B, C and D in Zone I | 44 |
| 4.5 | Electric field stress at point E, F, G and H in Zone II | 45 |
| 4.6 | Electric field stress at point I, J and K in Zone III | 47 |
| 4.7 | Electric field stress at point A, B, C and D in Zone I | 50 |
| 4.8 | Electric field stress at point E, F, G and H in Zone II | 52 |
| 4.9 | Electric field stress at point I, J and K in Zone III | 54 |
| 4.10 | Electric field stress at point A, B, C and D in Zone I | 57 |
| 4.11 | Electric field stress at point E, F, G and H in Zone II | 58 |
| 4.12 | Electric field stress at point I, J and K in Zone III | 60 |
| 4.13 | Electric field stress at point A, B, C and D in Zone I | 63 |
| 4.14 | Electric field stress at point E, F, G and H in Zone II | 64 |
| 4.15 | Electric field stress at point I, J and K in Zone III | 66 |

| | | |
|------|---|----|
| 4.16 | Electric field stress at point A, B, C and D in Zone I | 69 |
| 4.17 | Electric field stress at point E, F, G and H in Zone II | 70 |
| 4.18 | Electric field stress at point I, J and K in Zone III | 71 |
| 4.19 | Electric field stress at point A, B, C and D in Zone I | 74 |
| 4.20 | Electric field stress at point E, F, G and H in Zone II | 74 |
| 4.21 | Electric field stress at point I, J and K in Zone III | 74 |
| 4.22 | Dimension of proposed 132kV post insulator | 76 |
| 4.23 | Electric field stress at point A, B, C and D in Zone I | 81 |
| 4.24 | Electric field stress at point E, F, G and H in Zone II | 82 |
| 4.25 | Electric field stress at point I, J and K in Zone III | 82 |



LIST OF APPENDICES

| APPENDIX | TITLE | PAGE |
|-----------------|--|-------------|
| A | Base model of 132kV post insulator | 90 |
| B | Proposed model of 132kV post insulator | 91 |

LIST OF SYMBOLS AND ABBREVIATIONS

| | |
|----|------------------|
| kV | - Kilo Volt |
| DC | - Direct Current |
| cm | - Centimeter |
| mm | - Milimeter |



PTTA UTHM
PERPUSTAKAAN TUNKU TUN AMINAH

CHAPTER 1

INTRODUCTION

1.1 Introduction

The reliability of the power networks and equipments is very important for the performance of an electric power system. High voltage power lines have been widely used to transmit the electric energy from the power stations to the consumers. Insulators are among the important devices of the electric power transmission systems. They are used to support and separate conductors at high voltage. The insulators need to withstand not only regular voltages and overvoltages, such as lightning and switching events, but also various environmental stresses such as rain, snow and pollution [1, 2]. Presently insulators adopted for transmission/distribution are made of ceramic, glass or polymeric type. Ceramic and glass insulators have been used for a long time and there is considerable experience in manufacturing, installation and their field performance is well known.

Discharge activity on the surface of a high voltage insulator is caused by the local electric field having a value higher than the ionization level of the ambient air. This high electric field is the result of the applied voltage and the environmental conditions such as rain, pollution etc. If the surface electric field can be calculated or measured, it will be helpful to improve the insulator design through proper electric field grading techniques. At higher voltages, electric fields can be high enough to

cause surface flashover on ceramic/glass insulator, in case of polymeric type insulator damage to the insulator sheath due to the corona discharge; hence grading devices need to be used to reduce the electric field to acceptable levels [3].

1.2 Problem statement

Most of the insulators being used nowadays are of the ceramic and glass insulators considering their well known field performance. However, there is favorable improvement in the use of non-ceramic insulators which have shown advantages compared to ceramic and glass insulators such as low weight construction, good performance in contaminated environments and easy handling [4, 5]. Outdoor insulators are subject to electric stress and weather conditions such as rain, fog, heat and dew. The voltage and electric field near conductors is much higher than other area of the insulator, which may lead to corona discharge and even flashover. Therefore, study of electric field stress on a ceramic insulator when subject to a high voltage provides an important insight to improve the performance of the insulator. The design of a post insulator's plays an important role in the insulator's performance. The insulator's shed profile can affect the water collection on the insulator's surface and influence the electric field stress distribution along the insulator's surface. Moreover, the end fittings design is importance to ensure the occurrence of corona in the vicinity of end fitting on the insulator to be kept at minimum frequency as possible. A large number of electric field calculation software do exist that are based on different calculation methods, such as FDM (Finite Difference Method), FEM (Finite Element Method), BEM (Boundary Element Method), BIM (Boundary Integration Method) and CSM (Charge Simulation Method) [6-10]. In this project, the FEM (Finite Element Method) will be used to study the electric field surrounding the ceramic insulator when subject to high voltage. Optimized design of the insulator is needed to ensure the insulator can perform better and can provide longer service.

1.3 Objectives

The overall works of the project will stress on the study of the design of insulator. Several objectives are targeted from the work, such as:

- To investigate the electric field performance related to the insulator design.
- To propose an optimised design of insulator for controlling the electric field stress.

1.4 Scopes of the project

The 132kV post ceramic insulator will be modelled using finite element method (FEM) based software, COMSOL Multiphysics. In summary, several works have been identified such as:

- Literature review related to the work concept and the previous works by other researchers.
- Perform analytical study about the design of insulator.
- Simulation and analysis works on the existing and proposing optimised design model in term of electrical field stress performances.

CHAPTER 2

REVIEW OF LITERATURE

2.1 Overview

This chapter discussed about the overview of the studies on ceramic insulators, the electric field stress and the Finite Element Method (FEM). Past works and studies regarding to the design of insulator affecting the electric field strength are also reviewed.

Insulators are among the important devices of the electric power transmission system. Insulator is literally a very poor conductor. A true insulator is a material that does not respond to an electric field and completely resists the flow of electric charge. The function of the insulators can be seen from mechanical and electrical point of view. Their function is to support or separate electrical conductors without allowing current through themselves [11]. In this thesis, the insulator referred is of the ceramic post insulator type which has been used on electric power supply to support, separate or contain conductor at high voltage. Table 2.1 shows some of the project referred in completing this thesis along with their description.

Table 2.1 Journals referred in doing the project

| Author | Title of Project | Description |
|----------------------|--|--|
| E. Akbari et al. | Effects of Disc Insulator Type and Corona Ring on Electric Field and Voltage Distribution over 230-kV Insulator String by Numerical Method[12] | In this paper several 230-kV insulator strings with different porcelain and glass units were simulated using 3-D FEM based software, and their electric fields and voltage distributions were calculated and compared together, to investigate the effect of insulator types on these quantities. Tower and conductors were included in all simulations and also the effect of corona ring on voltage and electric field distribution over insulator strings with different insulator types was investigated. According to the results, distribution of voltage and electric field over insulator strings without corona ring and the degree of improvement of voltage distribution using corona ring depends on insulator material and profile, as well as the corona ring configuration parameters. Also tower existence and conductor length can change potential and electric field distributions extremely. |
| Ivanov, V. et al. | Enhancement Of Non-Ceramic Polymer Insulator Design Using Electrical Field Plot Analysis[13] | A commercially available software package is used to model insulators under a variety of applied voltages and contamination levels to establish relative electrical stresses. These stresses can be compared with designs that have been laboratory tested to verify an electrical performance improvement. The program was used to evaluate electrical stresses on insulators with different shed placements and profiles. Salt fog testing was conducted to determine the relationship between electrical performance and shed placement. The program was also used to evaluate electrical stress on insulators with different corona ring designs. |
| D. Cruz Dominguez | Optimization of Electric Field Grading Systems in Non-Ceramic Insulators[14] | Two electrical stress grading techniques for non-ceramic insulators are analyzed. In both techniques some parameters were optimized for a 115 kV non-ceramic insulator. Electric field simulations were performed with finite element method while, for the optimization process, different functions of the MATLAB 2011 optimization toolbox were used. In |

| | | |
|-------------------------|--|--|
| | | <p>the first case the optimized parameters were the relative permittivity of the material and the geometry of insulator on the energized side. The simulations were made under power frequency and under normalized lightning impulse. Modification of the shape next to the energized side consists of changing the inclination angle of the housing material. Furthermore, the corona ring position is optimized on the energized side of the non-ceramic insulator for comparison with the aforementioned method. According to the results, it was found that there are geometric parameters and material properties that minimize the value for the maximum electric field along the insulator surface.</p> |
| Xinqiao Wu et al | Calculation of Electric-field Distribution and Research on Characteristics of Shielding Ring along the Long-rod Post Porcelain Insulators Used in 1000kV System [15] | <p>In this paper, the finite element method is used to calculate the three-dimensional electric-field distribution of long-rod post porcelain insulators used in 1000kV system. The electric-field distribution is simulated in the condition of varied position, varied major radius and varied section dimension of the shielding ring. The effect of these factors to the external insulation characteristics of post porcelain insulators is analyzed. The electric-field distribution at the line side and the grounding flange can be effectively improved by proper distribution of shielding ring and the optimization of the shielding ring structure. This provide calculation gist to improve the characteristics of shielding ring used in 1000kV long-rod post porcelain insulators and the reliability of safe operation in 1000kV system.</p> |
| Edward Niedospial et al | Design and Application of Corona and Grading Rings for Composite Insulators[16] | <p>The addition of a corona ring to a polymer insulator will improve the insulators performance, but it must be the right ring used for the right reasons to realize the benefits. A corona ring should not be a quick fix to a problem; it may only mask a bigger concern or delay the inevitable. Selection of a corona ring is as critical a decision as picking the appropriate dry arc, leakage, or mechanical rating for the insulator. Beyond selecting the appropriate size ring for a</p> |

| | | |
|------------------------|---|--|
| | | specific voltage, other critical characteristics include attachment type, mating feature, hot stick-able design, ordering, and packaging |
| Ayman H. El-Hag et al. | Effect of Insulator Profile on Aging Performance of Silicone Rubber Insulators in Salt-Fog [17] | The paper presents the results of the study on the influence of insulator profile on the aging performance of silicone rubber (SIR) insulators in salt-fog. The work is also extended to include commercial 15 kV class insulators with different profiles. Shed spacing, shed diameter, alternate shed design and shed shape are the parameters investigated in this study. The low frequency harmonics of the leakage current, early aging period (EAP), and equivalent salt deposit density (ESDD), are used to evaluate the aging performance of different designs. Insulator profile is shown to greatly influence the aging performance of SIR insulators. Shed shape proves to be the most important parameter to be considered in designing non-ceramic insulators profiles. Also, as the shed spacing decreases, the performance of SIR insulators improves. Simulation results using FEMLAB show that the electric field on insulators is below the corona onset at both dry and wet conditions. Dry band arcing is therefore the main electrical cause for aging in distribution class insulators and it is possible to improve the pollution performance of SIR insulators using appropriate profiles as suggested in this work. |
| B. Vancia et al | Electric Field Modeling of Non-Ceramic High Voltage Insulators [18] | Electric field calculations are not common practice in the design and development of non-ceramic insulators for high voltage transmission applications. This paper applies a three-dimensional (3D) electric field analysis program to calculate the field distribution at the live-end of 275kV and 330 kV non-ceramic insulators used in the Queensland transmission system. At these voltages, fields can be high enough to cause damage to the insulator sheath due to corona discharge, and grading devices need to be used to reduce the electric field to acceptable levels. Of particular interest to this research was the |

| | | |
|-----------------|--|---|
| | | effect of end-fitting geometry and corona ring geometry on the electric field at the live-end of high voltage non-ceramic insulators. Three different non-ceramic insulator types were compared, and their fields are shown. Also a number of different ring geometries were compared. The effect of changing ring cross-sectional shape, diameter, and placement along the insulator are shown. All of these were found to influence the electric field at the live end. |
| Yang Qing et al | New Optimization Method on Electric Field Distribution of Composite Insulator [19] | Due to the geometry configure of composite insulator, the electric field strength near the two ends of composite insulator is always strong. The high electric field strength can cause the partial discharge on the insulation material and the surface of the metal electrodes, and bring premature aging of the insulator. In this paper, a new optimization method on the electric field distribution of composite insulator is put forward, which is the combined use of composite insulators and several units of glass insulator. Based on the finite element method, a three-dimensional electric field calculation model of insulators in the transmission line is established. Then the optimization conditions of surface potential and electric field distribution of composite insulator with glass insulator installed in the high voltage end of composite insulator at different levels of voltage is studied. The results show that by this method, the electric field distribution near the ends of composite insulators is significantly reduced, which can prevent the partial discharge and the aging of the composite material. |
| W. Sima et al | Optimization Of Corona Ring Design For Long-Rod Insulators Using FEM Based Computational Analysis [20] | The paper presents a method to optimize the location and the dimensions of the corona ring for transmission line composite insulators using finite element based software, FEMLAB. The procedure used to optimize the corona ring design, which handles more than one parameter, has been verified with examples that have an analytical solution or known optimal values. In this work the optimization is based on finding the maximum field along the |

| | | |
|---------------|--|--|
| | | insulator surface, such that this maximum field is well below the corona inception level. The design parameters of the ring diameter, diameter of the ring tube, position of the ring in its vertical plane, and the maximum field that cannot exceed the corona inception level have been used in the optimization process. |
| W. Sima et al | Study On The Shape Of Suspension Insulators Influencing Development Of Discharge[21] | Based on complex charge simulations method, this paper presents three-dimensional electrostatic models of suspension insulator with clearing pollution dry belt and appearing local arc along insulator surface. By calculating the electric field of suspension insulator surface, analyze the shape of suspension insulators influence to local arc development. It is studied that the relation between the shape of insulator and the development of local arc. The process of local arc development, the edge of suspension insulator influence greatly on the development of local arc. The results can provide theory basis for informing the shape of insulator. |

2.2 Ceramic insulator

Ceramic insulators are still widely used worldwide although they were the first type of insulator invented. They have proven to give excellent service history backed by years of manufacturing experience from reputable firms. Figure 2.1 shows the example of ceramic insulators. The basic components used to make the ceramic insulator are clay, fine sand quartz and feldspar. Ceramic insulators can be divided into two types namely porcelain and glass. Porcelain and glass give a little difference regarding to their cost and performance. Toughened glass has the advantage for overhead lines that upon impact the broken insulators tend to shatter completely and therefore are easily spotted during maintenance inspections. On the other hand, the glass insulators are rarely used in substation practice since they leave only some 15mm between the top metal cap and the pin upon shattering. Porcelain insulators which may be chipped or cracked, but not

shattered are therefore preferred for substation use since access for replacement may require a busbar outage [22]. The design and manufacturing of the ceramic insulators are being researched and improved in order to cater the needs of today's power distribution and transmission system. However, limitations are given on their sheds design to meet the surface electrical leakage distance needed for higher voltage transmission. To smooth the surface of the insulator, glazing is used apart from increasing the mechanical strength and improving the surface's hydrophobicity.

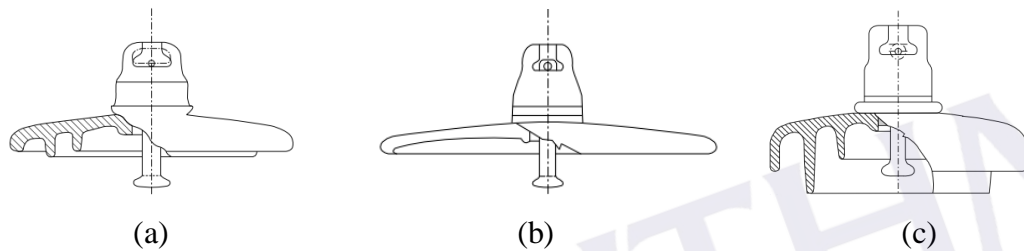


Figure 2.1 Typical constructions of ceramic type suspension insulators. (a) Standard.

(b) Open profile (self-cleaning). (c) Anti-fog and for DC applications [34]

2.3 Electric field stress

It is important to understand the electric field intensity in high voltage engineering to design an insulator that could provide long and satisfactory performance. Electric stress is the stresses upon the dielectric by electric field which is produced due to the potential on the dielectric. The electric field intensity is the parameter used to determine the magnitude of the electric field stress on the dielectric. The performance of a dielectric depends strongly on the electric field distribution and the electric field stress.

The electric field intensity or known the electric field strength is defined as the electrostatic force, F per unit positive test charge, q placed at a particular point p in a dielectric [22]. It is denoted by E , and expressed in the unit “Newton per Coulomb”, that is, the force per unit charge. Since the potential is expressed in “Joules per Coulomb (J/C)”, or “Newton-meter per Coulomb (Nm/C)”, which is defined as “Volt”, the

electric field intensity is measured in its more common practical units of “Volt per meter” (V/m or kV/cm). The electric field intensity is often called as the electric field stress experienced by a dielectric.

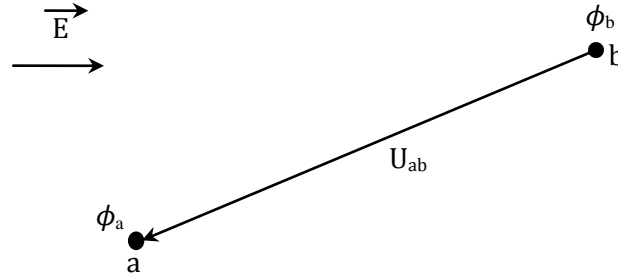


Figure 2.2 Illustration of electric field

In Figure 2.2, the potential difference U_{ab} between two points **a** and **b** having scalar potential ϕ_a and ϕ_b in an electric field, \vec{E} , is defined as the work done by an external source in moving a unit positive charge from **b** to **a**.

$$U_{ab} = - \int_b^a |\vec{E}| dx = (\phi_a - \phi_b) \quad (2.1)$$

The magnitude of electric field intensity is given by the rate of change of potential with distance. The maximum magnitude of the field intensity is obtained when the direction of \vec{E} is opposite to the direction in which the potential is increasing most rapidly,

$$\left. \frac{dU_{ab}}{dx} \right|_{max} = -|\vec{E}|_{max} \quad (2.2)$$

Equation (2.2) provides a physical interpretation of the process of finding electric field intensity from the scalar potential ϕ . The operator on ϕ by which \vec{E} is obtained is thus known as the gradient. The relationship between ϕ and \vec{E} is written as,

$$\vec{E} = -\nabla \phi \quad (2.3)$$

2.4 Numerical electric field analysis methods

A comprehensive reference book related to numerical electric field analysis methods is authored by Zhou [23]. There are several numerical analysis methods that are often used for the calculation of the electric field strength distribution along insulators. They are:

- charge simulation method (CSM)
- boundary element method (BEM)
- finite element method (FEM)
- finite difference method (FDM).

The numerical electric field analysis methods can be divided into two categories: the boundary methods and the domain methods. The boundary methods include the CSM and the BEM. The domain methods include the FEM and the FDM. Table 2.2 shows a brief explanation of each numerical method used to approximate the electric field strength distribution.

Table 2.2 Brief explanation on the numerical method to calculate electric field

| Method | Description |
|--------|--|
| CSM | The basic concept of the CSM is to replace the distributed charge of conductors and the polarization charges on the dielectric interfaces by a large number of fictitious discrete charges. The magnitudes of these charges have to be calculated so that their integrated effect satisfies the boundary conditions. The potential due to unknown surface charges can be approximated by three forms of concentrated fictitious charge arrangements – line, ring and point charges [24]. These charges can be placed at appropriate positions, which are usually inside the conductor surfaces. An adequate combination of the three forms of charges can be made to simulate almost any practical electrode system. The CSM method can be used to solve open boundary problems and is easily applied for three-dimensional electric field problems without axial symmetry. A major problem of CSM is the difficult and subjective |

| | |
|-----|---|
| | placement of simulation charges. The other disadvantage is that it is difficult or impossible to calculate the electric field strength near very thin electrodes because the fictitious charges approximating the field must be usually inside the electrodes. |
| BEM | The BEM is based on the boundary integral equation and the principle of weighted residuals, where the fundamental solution is chosen as the weighting function. There are two kinds of BEM. One is called indirect BEM, the other is called direct BEM. In the indirect BEM, the potential is not solved directly. An equivalent source, which would sustain the field, is found by forcing it to satisfy prescribed boundary conditions under a free space Green function that relates the location and effect of the source to any point on the boundary. Once the source is determined, the potential or derivatives of the potential can be calculated at any point |
| FEM | The FEM is a numerical method of solving Maxwell's equations in the differential form. The basic feature of the FEM is to divide the entire problem space, including the surrounding region, into a number of non-separated, non-overlapping subregions, called "finite elements". This process is called meshing. These finite elements can take a number of shapes, but generally triangles are used for 2-D analysis and tetrahedron for 3-D analysis. Each element geometry is expressed by polynomials with nodal values as coefficients. The electric potential within each element is a linear interpolation of the potentials at its vertices. By using the weighted residual approach, the partial differential equations are reduced to a sparse, symmetric and positive definite matrix equation. Since the shape and the size of the elements are arbitrary, it is a flexible method that is well suited to problems with complicated geometry. The FEM analysis is effective for small problems that are closed bounded. If the problems are too large, a large number of finite elements are required, and the calculation becomes intensive. |
| FDM | The FDM is an approximate method for solving partial differential equations. It replaces a continuous field problem by a discretized field |

| | |
|--|---|
| | with finite regular node. This method utilizes a truncated Taylor series expansion in each coordinate direction, and applied at a set of finite discretization points to approximate the partial derivatives of the unknown function. The partial differential equations are transformed into a set of algebraic equations. The FDM is suitable for obtaining an approximate solution within a regular domain. If a region contains different materials and complex shapes, the FEM is better than the FDM. |
|--|---|

2.4.1 Finite element method

Finite Element Method (FEM) [25] in general is based on transforming the differential equations in integral form and then using an approximation. One way to transform these equations is to find a function that minimizes an energy integral. An easy way to calculate the electric field distribution is to calculate electric potential distribution initially and then calculate field distribution by subtracting gradient of electric potential distribution from it [26]. From equation (2.3),

$$\vec{E} = -\nabla \phi$$

From Maxwell's equation,

$$\nabla \cdot \vec{E} = \frac{\rho}{\epsilon} \quad (2.4)$$

where ρ is the volume charge density, ϵ is the permittivity of dielectric material ($\epsilon = \epsilon_0 \epsilon_r$), ϵ_0 is vacuum permittivity, (8.854×10^{-12}) and ϵ_r is the relative permittivity of dielectric material. The Poisson's equation can be obtained by substituting equation (2.4) into equation (2.3)

$$\nabla^2 \phi = -\frac{\rho}{\epsilon} \quad (2.5)$$

The Laplace's equation can be obtained by making space charge $\rho = 0$,

$$\nabla^2 \phi = 0 \quad (2.6)$$

The basic approach of FEM for electric field estimation involves the factual characteristics of an electrostatic field that the total energy enclosed in the whole field region acquires a minimum value. In other words, the potential, ϕ , under given conditions of electrode surface, should make the enclosed energy function to be at a minimum for a given dielectric volume “V”, therefore:

$$W = \int_V \frac{1}{2} \epsilon (\nabla \phi)^2 dV \rightarrow \text{minimum} \quad (2.7)$$

which is obtained by solving the basic potential equation (2.3). W is the electrical energy stored in the volume of dielectric under consideration.

Hence, in this method the field between the electrodes under consideration is subdivided into finite number of discrete sized elements. The behavior of these elements is specified by a number of parameters, for example, the potential. The number of nodal points and elements established within the mesh are assigned identifying integer numbers. The shape of these discrete elements is suitably chosen to triangular for two dimensional representations. For three dimensional field configurations, “tetrahedron”, a pyramid-like solid structure with four plane triangular faces, shown in Figure 2.3, is used.

The size and the orientation of the triangles, as well as the tetrahedrons, irregularly distributed over the generated mesh in the field region depending upon the magnitude of the potential gradient. At the locations where higher field intensity or electric-stress exists, discrete elements of smaller size cover the region.

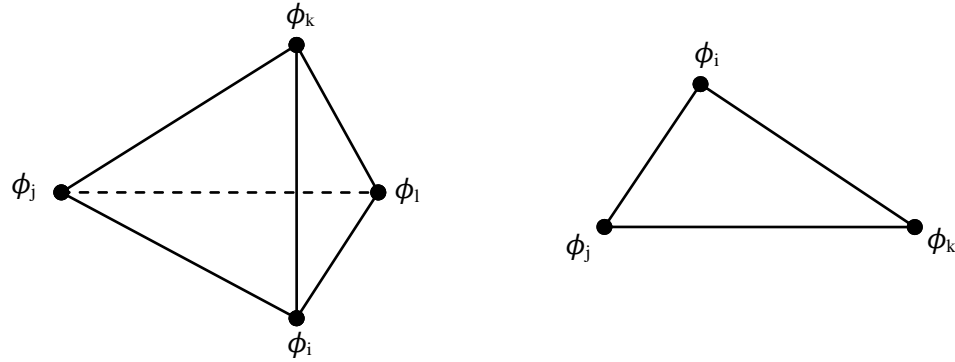


Figure 2.3 Triangular and tetrahedron shaped finite discrete elements.

Consider an electrostatic field, undistorted by any space charge concentration, in a single isotropic dielectric between two electrodes. Then the potential ϕ would be determined by the boundaries, that is, the metal electrode surfaces. The above equation (2.7) for electrical energy W , stored within the whole region of such a Laplacian field is given in Cartesian coordinates as follows,

$$W = \iiint_V \left[\frac{1}{2} \varepsilon \left\{ \left(\frac{\delta \phi}{\delta x} \right)^2 + \left(\frac{\delta \phi}{\delta y} \right)^2 + \left(\frac{\delta \phi}{\delta z} \right)^2 \right\} \right] dx dy dz \quad (2.8)$$

For a small volume element $dV = (dx dy dz)$, the expressions $(1/2 \varepsilon \Delta^2 \phi)$ within equation (2.8) represent the energy densities per unit volume in a particular direction.

For two dimensional case, it is assumed that the potential distribution does not change in the z direction. Then, the total energy W_A stored within the area A per unit length located between the two electrodes boundaries can be given by the equation (2.7)

$$W_A = \int_A \frac{1}{2} \varepsilon (\nabla \phi)^2 dA$$

And according to equation (2.8) in this case by,

$$W = z \iint_A \left[\frac{1}{2} \varepsilon \left\{ \left(\frac{\delta \phi}{\delta x} \right)^2 + \left(\frac{\delta \phi}{\delta y} \right)^2 \right\} \right] dx dy \quad (2.9)$$

where z is a constant. W/z gives the energy densities per elementary area dA . Inside each sub-domain, a linear dependency of ϕ on x and y is assumed, which gives rise to the first order approximation,

$$\phi(x, y) = \phi = a_{e1} + a_{e2}x + a_{e3}y \quad (2.10)$$

Where ϕ is the electrical potential of any arbitrary point inside each sub-domain, a_{e1} , a_{e2} , a_{e3} are the computational coefficients for a triangle element e , and m is the total number of triangle elements. Equation (2.10) implies that within the element the potential are linearly distributed and the field intensity is constant.

In order to minimize the energy within the field region under consideration, only derivatives of the energies with respect to the potential distribution in each element are of particular interest. For element under consideration, W_e is the energy enclosed within the element, then the energy per unit length W_e/z in the direction z , denoted by $W_{\Delta e}$ can be given as follows,

$$W_{\Delta e} = \frac{W}{z} = \frac{1}{2} \Delta_e \varepsilon \left[\left(\frac{\delta \phi}{\delta x} \right)^2 + \left(\frac{\delta \phi}{\delta y} \right)^2 \right] \quad (2.11)$$

The symbol Δ_e represents the area of the discrete triangular element under consideration. If we denote the total energy in the whole field of given elements by W_{Δ} , the relation for minimizing the energy within the complete system can be given as,

$$\frac{\partial W_{\Delta}}{\partial \{\phi\}} = 0 \quad (2.12)$$

where $\{\phi\}$ is the total potential vector for all the nodes within a given system. The final matrix expression is

$$\frac{\partial W\Delta}{\partial \{\phi\}} = 0 = [H]\{\phi\} \quad (2.13)$$

where the matrix $[H]$ is known as the “stiffness matrix”. The above matrix is solved by iterative methods.

2.5 Factors influencing the electric field stress on insulator.

Previous studies proved that other design parameters than the creepage distance may be critical for the short and long term performance of insulators. This section provides brief explanation on the factors that affect the electric field stress on insulator.

2.5.1 Shape of insulator

The shape of the insulator plays a significant role in determining the electric field stress along the insulator. A good design of insulator must provide electrical field stress below ionization threshold. Weather shed profile and the end fitting design are the aspect of interest to control the electric field stress on insulator.

a) Weather shed profile

The shed profile is a parameter that needs to be studied. The shed profile should be aerodynamic in shape. Based on the previous studies, the electric field strength is significantly higher in the sheath/shed transition area than in adjacent areas. The influence of the rounding radius of the sheath/shed transition area on the electric field distribution along the insulators is of interest.

Chakravorti and Steinbigler [32] studied the relationship between the shape of a porcelain post-type insulator and the maximum electric field strength around it with or without pollution. The position of the maximum electric field strength is near the top triple junction region. The parameters studied in their work are the slope angle of the insulator weather shed, the shed radius, the core radius, the axial height, and the electrode radius. Their findings were as follows:

- The higher slope angle does not yield notable reduction in the maximum electric field strength.
- Increasing the shed radius from 6 cm to 10 cm significantly lowers the maximum electric field strength.
- The increase of the core radius has little effect on the maximum electric field strength reduction.
- The higher the axial height, the lower the maximum electric field strength.
- For a given insulator shape, increasing the electrode radius increases the maximum electric field strength in clean conditions but reduces the maximum electric field strength in the presence of surface pollution.

b) End fitting design

End-fitting geometry was also found to have a significant influence on the electric fields around the energized end. In [28], simulations were carried out on three insulator fitting types, without the presence of a corona ring in the model. Large end fitting with rounded edges tend to reduce the peak magnitude of the electric field strength values in close proximity of the end fitting. Furthermore, the end fitting with bigger diameter was found to have better electric field stress distribution in the vicinity of the end fitting. Figure 2.4 shows the three different fittings and the contour maps associated with each fitting.

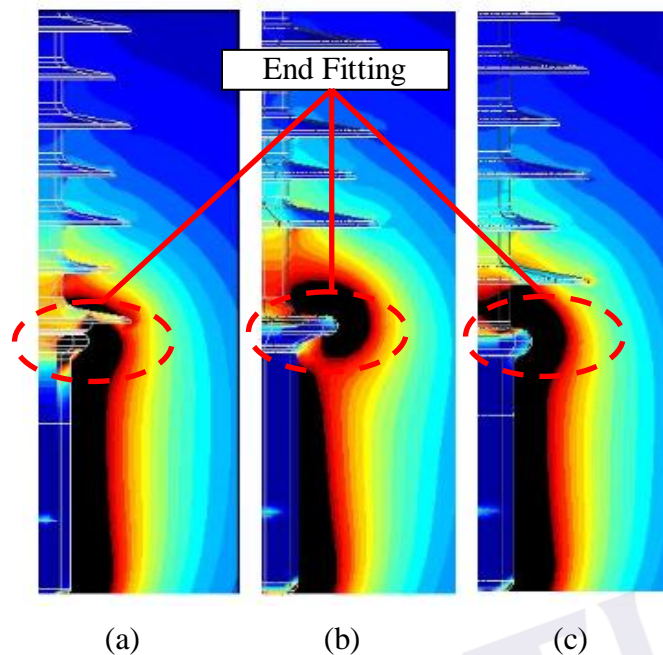


Figure 2.4 Examples of the electric field distribution surrounding the composite insulator end fitting of (a) Design 1 (b) Design 2 and (c) Design 3[28]

2.5.2 Corona ring application

The function of the corona ring is to grade or disperse the electric field gradient, thus reducing the voltage stress on the rubber housing near the line end fitting. The corona ring can be attached to the composite insulator directly or as part of the hardware. When applied as part of the hardware, the grading device is commonly referred to as a Corona Shield. Corona rings are typically used to prevent inception of corona on hardware. Figure 2.5 shows the difference of the electric field distribution with the application of corona ring.

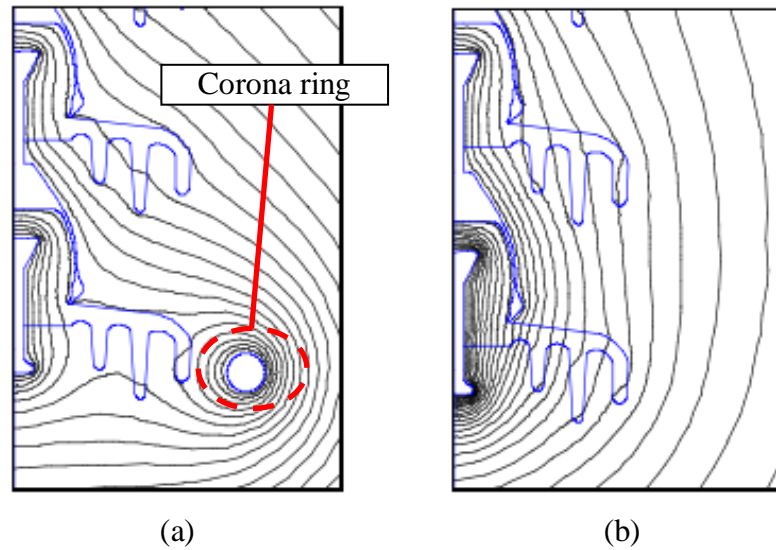


Figure 2.5 Potential distributions on insulator (a) with corona ring and (b) without corona ring [27]

Suat İlhan and Aydoğan Özdemir [27] studied the effect of corona ring application to the electric field stress and potential distribution along insulator. They found that the usage of corona ring in an insulator string will significantly decrease the voltage percentage on the lowermost insulators and will slightly increase the voltage sharing on the uppermost insulators. That is, potential distribution will be more uniform with the help of corona ring. Furthermore, the maximum electric field strengths on the live end side will importantly decrease with the usage of corona ring. The value of this field strength depends on the corona tube settings. On the basis of vertical position of corona ring, electric field on the live end gets its minimum value. Moreover, the electric field on the corona ring surface can also change with the design parameters. Maximum electric field is on the outer radius of the ring. However, minimum electric field is on the inner radius of the ring.

Zhao and Comber [31] studied the electric field and potential distribution along non-ceramic insulators. The Coulomb electric field analysis software was used. The insulator, tower and conductors were considered in the calculation model. Results showed that the conductor length has significant “shielding” effect on the insulators; the maximum electric field strength decreases when the length of the conductor increases; and the tower structure in the vicinity of the insulator and the diameter and the location

of the grading ring are important in determining the maximum electric field strength along an insulator.

2.5.3 Permittivity of the material

Permittivity (ϵ) is a measure of how an electric field affects, and is affected by, a dielectric medium. The permittivity of a medium describes how much electric field, or more correctly, fluxes, is generated per unit charge. Less flux exists in a medium with a high permittivity due to polarization effects. Permittivity is directly related to electric susceptibility, which is a measure of how easily a dielectric polarizes in response to an electric field.

Kaana-Nkusi, Alexander and Hackam [29] calculated the voltage and electric field distribution along a post-type insulator shed. The system was modeled with 146 ring charges, with 30 charges modeling each electrode. Several criteria were applied in order to evaluate the quality of the calculation results, which included the potential error, the potential discrepancy, the normal electric flux density and the tangential electric field strength discrepancies. The calculation results showed that the maximum values of the electric field strength along the surface increased with higher dielectric permittivity of the insulating material. Decreasing the radius of curvature of the insulator shed increased both the normal and tangential components of the electric field strength. Table 2.3 shows some example of permittivity of material.

Table 2.3 Relative permittivity of material [36]

| Material | Relative permittivity |
|----------------|-----------------------|
| Air | 1 |
| Porcelain | 5.0-7.0 |
| Water | 4.0-8.0 |
| Silicon rubber | 3.2-9.8 |

2.5.4 Potential difference

The potential difference applied on an insulator also affects the electric field stress on the insulator. The electric field is a measure of force per unit charge and the electric potential is a measure of energy per unit charge. Let say a work done in moving a unit test charge from point *a* to point *b* is the electric potential difference between the two points and is denoted by ΔV and Δd is the distance needed to move the charge. Therefore, the relation between potential difference and field strength can be given as

$$\vec{E} = - \frac{\Delta V}{\Delta d}$$

The negative sign indicates that the potential decreases in the direction of electric field.

2.5.5 External influences

High voltage insulators often work outdoors, which are affected by adverse environmental and atmospheric factors, such as dust, fog, dew, rain, snow and other industrial pollution. When the air humidity is lower, the existence of these contaminations will not affect the normal work of the insulator. But when the air humidity is higher, the contamination layers on the surface of the insulators will be wet, and the soluble salt of the contaminations will be dissolved in water. The conductive water film is formed which leads to the higher conductance of the insulator surface. Then the leakage current increases sharply, and the flashover voltage of the insulators reduces greatly. Because of this, the flashover can occur in the operating voltage. Many researches about the insulator surface electric field under contamination distribution indicate that the distribution of the contaminations on the insulator surface affects the

insulator surface electric field greatly, and the occurrence of flashover is closely related to the distribution of the electric field and potential.

2.6 Effect of electric field stress on insulator

This section will describe about the effect of high electric field stress on insulator. Specifically, the event of corona discharge, flashover and discharge activity on the insulator will be discussed.

2.6.1 Corona discharge

Corona discharges occur on the surface when electric field intensity exceeds the breakdown strength of air, which are around 15 kV/cm. Atmospheric conditions which effect corona generation are air density and humidity. The geometry of insulator itself has a role in the initiation of corona activity. The corona generates ultraviolet light, heat, and gaseous by products (ozone, NO₂). The corona discharges subject the insulator to severe electrical strains and chemical degradation. Continued degradation may render the ceramic insulator ultimately unusable. When corona generation occurs on a wet surface, this results in 'wetting corona activity'. Wetting corona activity is the outcome of a non-uniform wetting causing high electric field. This activity depends on the type and magnitude of wetting as well as on the intensity of surface electric field. The magnitude of wetting depends on the surface characteristics (hydrophobic or hydrophilic) and on the type of wetting whether it is produced by rain, mist, fog or condensation. Magnitude of surface electric field depends upon the dimension of grading ring, its position and end fittings.

Wetting corona activity occurs mainly at live and ground terminals. Lower hydrophobicity makes discharge activity more likely. Besides the undesirable effect

REFERENCES

- [1] Andy Schwalm, "Insulators 101", *IEEE/PES 2010 Transmission and Distribution Conference and Exposition*, 2010.
- [2] Subba Reddy, B.; Ravishankar, K.V.; Sultan, N. A. et al, "Simulation of Potential and Electric Field for High Voltage Ceramic Disc Insulators", *2010 5th International Conference on Industrial and Information Systems, (ICIIS 2010)*, pp. 526 – 531, 2010.
- [3] Kojimi, S.; Oyama, M.; Yamashita, M., "Potential Distribution Of Metal Oxide Surge Arresters Under Various Environmental Conditions," *IEEE Trans. on Power Delivery*, Vol. 3, No.3, pp 984-989, 1988.
- [4] Phillips, A., "Electric Field Distribution And Their Impact On Transmission Line Composite Insulators", *IEEE Power Eng. Soc. (PES) Transmission and Distribution Conf. and Exposition (T&D)*, Charlotte, NC, pp. 1-3, 2012.
- [5] Gorur, R. S.; Cherney, E. A.; Burnham, J. T., *Outdoor Insulators*: Ravi S. Gorur, Inc., ISBN 0967761107, 1999.
- [6] Cigre working group 22.03, "Comparative Electric Field Calculations and Measurements on High Voltage Insulators", *Electra* No. 141, pp. 6977, April 1992.
- [7] Chakravorti, S.; Mukerjee, P. K., "Power Frequency And Impulse Field Calculations Around A HV Insulator With Uniform Or Non-Uniform Surface Pollution", *IEEE Trans on Dielectrics and Electrical insulation*, Vol. 28, No.1, pp 43-53, Feb 1993.
- [8] Chakravorti, S.; Steinbigler, H., "Capacitive resistive field calculation on HV bushing using the boundary element method", *IEEE Trans. On Dielectrics and Electrical Insulation*, Vol. 5, No.2, pp 237-244, April 1998.

- [9] Andersen, O. W., "Finite element solution of complex electric fields", *IEEE Trans. on PAS*, Vol. 96, No.4, pp 1156-1160, 1977.
- [10] El Kishky, H.; Gorur, R. S., "Electric potential and field computation along ac HV insulators", *IEEE Trans. on Dielectrics and Electrical Insulation*, Vol.1, No.6, pp 982-990, Dec 1994.
- [11] Cotton, H., *The Transmission and Distribution of Electrical Energy*: Hodder and Stoughton, ISBN 0340147717, 1978.
- [12] E. Akbari et al, "Effects of Disc Insulator Type and Corona Ring on Electric Field and Voltage Distribution over 230-kV Insulator String by Numerical Method", *Iranian Journal of Electrical & Electronic Engineering*, Vol. 9, No. 1, March 2013.
- [13] Ivanov, V. et al, "Enhancement Of Non-Ceramic Polymer Insulator Design Using Electrical Field Plot Analysis", *Electrical Electronics Insulation Conference*, pp. 437-441, Sep 1995.
- [14] Dominguez, D.C.; Espino-Cortes, F.P.; Gomez, P., "Optimization of Electric Field Grading Systems in Non-Ceramic Insulators", *Electrical Insulation Conference (EIC)*, pp. 231-234, June 2011 .
- [15] Xinqiao Wu ; Zongren Peng ; Peng Liu ; Zhong Yu, "Calculation of Electric-field Distribution and Research on Characteristics of Shielding Ring along the Long-rod Post Porcelain Insulators Used in 1000kv System" *Properties and applications of Dielectric Materials, 8th International Conference*, pp. 603-606, June 2006.
- [16] Niedospial, E. , "Design and Application of Corona and Grading Rings for Composite Insulators", *Transmission and Distribution Conference and Exposition (T&D), IEEE PES*, pp. 1-3, May 2012.
- [17] El-Hag, A.H. ; Jayaram, S.H. ; Cherney, E.A. , "Effect of Insulator Profile on Aging Performance of Silicone Rubber Insulators in Salt-Fog", *Dielectrics and Electrical Insulation, IEEE Transactions*, Vol 14, No. 2, pp. 352 – 359, April 2007.
- [18] Saha, T. K.; Eleperuma, K.; Gillespie, T., "Electric Field Modeling of Non-Ceramic High Voltage Insulators", University of Queensland & Powerlink.
- [19] Yang Qing; Wenxia Sima; Deng Jiazhao; Yuan Tao; Chen Lin, "New Optimization Method on Electric Field Distribution of Composite Insulator",

Electrical Insulation and Dielectric Phenomena (CEIDP) Annual Report Conference, pp. 1-4, Oct 2010.

- [20] Sima, W.; Espino-Cortes, F.P.; Cherney, E.A.; Jayaram, S.H., "Optimization of Corona Ring Design for Long-Rod Insulators Using FEM Based Computational Analysis", *Conference Record of the 2004 IEEE International Symposium on Electrical Insulation*, pp. 480-483, Sept 2004.
- [21] Wenxia Sima; Caixin Sun; Leguan Gu; Xinliang Jiang; Mingying Chen, "Study On The Shape Of Suspension Insulators Influencing Development Of Discharge", *International Symposium on Electrical Insulating Materials (ISEIM)*, pp. 290-292, Nov 2001.
- [22] Bayliss, C.; Hardy, B., *Transmission and Distribution Electrical Engineering 4th edition*: Elsevier, ISBN 0080969135, 2011.
- [23] Zhou P. B., *Numerical Analysis of Electromagnetic Fields*. Springer-Verlag, Berlin, ISBN 0387547223, 1993.
- [24] Khan, M. J.; Alexander, P. H., "Charge Simulation Modeling of Practical Insulator Geometries," *IEEE Transactions on Electrical Insulation*, Vol. EI-17, No. 4, August 1982, pp. 325-332.
- [25] Arora, R.; Mosch, W., *High Voltage and Electrical Insulation Engineering Volume 69 of IEEE Press Series on Power Engineering*: John Wiley & Sons, ISBN 1118008960, 2011.
- [26] Muniraj, C.; Chandrasekar, S., "Finite Element Modeling For Electrical Field And Voltage Distribution Along The Polluted Polymeric Insulator", *World Journal of Modelling and Simulation*, Vol. 8, No. 4, pp. 310-320, March 2012.
- [27] Suat Ilhan; Aydogan Özdemir, "Effect of Corona Ring Design on Electric Field Intensity and Potential Distribution Along an Insulator String," *IEEE ELECO*, 2007.
- [28] Phillips, A. J. et al, "Electric Field on AC Composite Line Insulators", *IEEE Transactions On Power Delivery*, Vol. 23, No. 2, pp. 823-830, April 2008.
- [29] Kaana-Nkusi, S.; Alexander, P. H.; Hackam, R., "Potential and Electric Field Distributions at a High Voltage Insulator Shed," *IEEE Transactions on Dielectrics and Electrical Insulation*, Vol. 23, No. 2, pp. 307-318, April 1988.

- [30] Gutfleisch, F.; Singer, H.; Forger K.; Gomollon, J. A., "Calculation of High Voltage Fields by Means of the Boundary Element Method", *IEEE Transactions on Power Delivery*, Vol. 9, No. 2, pp. 743-749, April 1994.
- [31] Zhao, T.; Comber, M. G., "Calculation of Electric Field and Potential Distribution Along Non-Ceramic Insulators Considering the Effects of Conductors and Transmission Towers," *IEEE Transactions on Power Delivery*, Vol. 15, No. 1, pp. 313-318, January 2000.
- [32] Chakravorti, S.; Steinbigler, H., "Boundary-Element Studies on Insulator Shape and Electric Field around HV Insulators with or without Pollution", *IEEE Transactions on Dielectrics and Electrical Insulation*, Vol. 7, No. 2, pp. 169-176, April 2000.
- [33] COMSOL, "Introduction to COMSOL Multiphysics", May 2013.
- [34] Edmund Kuffel, Walter S. Zaengl, John Kuffel, *High Voltage Engineering Fundamentals*: Butterworth-Heinemann, ISBN 0750636343, 2000.
- [35] Schumann, U. et al, "FEM Calculation and Measurement of the Electrical Field Distribution of HV Composite Insulator Arrangements", *39th CIGRE Session*, August 2002.
- [36] Clipper Controls, "Dielectric Constant Value," [Online] Available from: <http://www.clippercontrols.com/pages/Dielectric-Constant-Values.html#V> [Accessed 26 September 2013].
- [37] Powerline Patrol Services, "UV Corona," [Online] Available from: <http://www.powerlinepatrol.com/patrol-services/our-technology/uv-corona/> [Accessed 6 March 2013].